HHS Public Access

Author manuscript

Exp Cell Res. Author manuscript; available in PMC 2019 January 03.

Published in final edited form as:

Exp Cell Res. 2018 June 15; 367(2): 150–161. doi:10.1016/j.yexcr.2018.03.031.

Connexin 43 regulates the expression of wound healing-related genes in human gingival and skin fibroblasts

Rana Tarzemany[a], **Guoqiao Jiang**[a], **Jean X. Jiang**[b], **Corrie Gallant-Behm**[c], **Colin Wiebe**[a], **David A. Hart**[d], **Hannu Larjava**[a], and **Lari Häkkinen**[a,*]

[a]Department of Oral Biological and Medical Sciences, Faculty of Dentistry, The University of British Columbia, Vancouver, BC, Canada V6T 1Z3

[b]Department of Biochemistry and Structural Biology, University of Texas Health Science Center, San Antonio, TX 78229-3900, USA

[c]miRagen Therapeutics, Inc., Boulder, CO, USA

[d]Department of Surgery, McCaig Institute for Bone and Joint Health, University of Calgary, Calgary, Alberta, Canada

Abstract

Fibroblasts are the most abundant connective tissue cells and play an important role in wound healing. It is possible that faster and scarless wound healing in oral mucosal gingiva relative to skin may relate to the distinct phenotype of the fibroblasts residing in these tissues. Connexin 43 (Cx43) is the most ubiquitous Cx in skin (SFBLs) and gingival fibroblasts (GFBLs), and assembles into hemichannels (HCs) and gap junctions (GJs) on the cell membrane. We hypothesized that SFBLs and GFBLs display distinct expression or function of Cx43, and that this may partly underlie the different wound healing outcomes in skin and gingiva. Here we show that Cx43 distinctly formed Cx43 GJs and HCs in human skin and gingiva *in vivo*. However, in SFBLs, in contrast to GFBLs, only a small proportion of total Cx43 assembled into HC plaques. Using an *in vivo*-like 3D culture model, we further show that the GJ, HC, and channel-independent functions of Cx43 distinctly regulated wound healing-related gene expression in GFBLs and SFBLs. Therefore, the distinct wound healing outcomes in skin and gingiva may partly relate to the inherently different assembly and function of Cx43 in the resident fibroblasts.

*Correspondence to: The University of British Columbia, Faculty of Dentistry, Department of Oral Biological and Medical Sciences, 2199 Wesbrook Mall, Vancouver, BC, Canada V6T 1Z3. lhakkine@dentistry.ubc.ca (L. Häkkinen).

Author contributions statement

Conceived and designed the experiments: RT, GJ, LH. Performed the experiments: RT, GJ. Analyzed the data: RT, LH. Contributed reagents/materials/analysis tools: HL, LH.

Wrote the main manuscript text and analyzed the results: RT, GJ, HL, LH. Developed and affinity purified the Cx43(E2) antibody: JXJ. Participated in the pig experiment: CG-B, CW, DH, HL, LH. All authors reviewed the manuscript

Competing interests statement

All authors declare that there are no competing interests.

Disclosures

C.G.-B. is a full-time employee and holds stocks and stock options for miRagen Therapeutics, Inc.

Appendix A. Supporting information

Supplementary data associated with this article can be found in the online version at http://dx.doi.org/10.1016/j.yexcr.2018.03.031.

Keywords

Skin; Gingiva; Fibroblasts; Connexin 43; Gap junctions; Hemichannels

1. Introduction

Fibroblasts are a heterogeneous and abundant group of connective tissue cells. Such cells play a key role in wound healing and scar formation by regulating ECM production and remodeling, inflammation, angiogenesis and reepithelialization [22,27,43]. Accumulating evidence indicates that the outcome of a wound may depend on the phenotype of the fibroblasts in a given tissue. For example, gingiva, which is characterized by fast and significantly reduced scar-forming wound healing as compared to skin [20,42,49,68,78], harbors fibroblasts with a phenotype and regenerative potential that is distinct from adult skin fibroblasts [20,28,53]. Human gingival fibroblasts (GFBLs) display a gene expression pattern that is less pro-fibrotic than do skin fibroblasts (SFBLs) [19,47,48]. GFBLs also migrate faster into the early provisional wound matrix and degrade it quicker than SFBLs, another factor which may contribute to efficient gingival wound healing [46]. Some suggest that this difference in GFBLs and SFBLs may derive from their different developmental origins. Most of GFBLs may originate from neural crest. In contrast, fibroblasts in trunk and limb dermis derive from somites and lateral plate mesoderm [28,43,72,81]. Thus, the distinct phenotypic properties of GFBLs and SFBLs may underlie the different wound healing outcomes in these tissues.

Connexins (Cxs) are a family of 21 transmembrane proteins that play an integral role in wound healing [67]. However, very little is known regarding their expression and function in GFBLs compared to SFBLs *in vivo* or *in vitro*. Each Cx protein contains four transmembrane domains with two extracellular loops, one cytoplasmic loop, and N- and C-terminal intracellular domains. Assembly of six Cx subunits forms a hemichannel (HC), establishing a conduit for the transfer of small ions and signaling molecules between the cell cytosol and the extracellular environment. Head-to-head docking of two HCs from neighboring cells forms a gap junction (GJ), which provides direct cell-to-cell contact for communication via the exchange of small (< 1 kDa) molecules [32,35]. Typically, Cx GJs and HCs cluster in large plaques on cell membranes, and these plaques can be detected by immunostaining [4,41,70].

In general, channel functions of both HCs and GJs are regulated by similar factors although, interestingly, they are often affected in opposing manners. For example, while increased levels of inflammatory cytokines, elevation of intracellular Ca^{2+} concentration or oxidative stress promote the opening of HCs during wound healing or ischemia, they may also induce closure of GJs [32,61]. Cx HCs and GJs also distinctly regulate various cell functions including proliferation, migration, death, survival, wound healing, and gene expression [5]. Cxs can also regulate gene expression, cell adhesion, migration, and apoptosis through functions that are not related to the Cx channel functions, but instead involve interactions of Cx43 cytoplasmic domains with other cytoplasmic signaling molecules. These channel-independent functions of Cxs are still not completely understood [33,52,83].

Cx43 is the most ubiquitous Cx in skin and gingiva, and its expression is dynamically regulated during wound healing in these tissues. In skin, Cx43 also regulates the wound healing process [9,69]. For instance, compared to normal skin, Cx43 is strongly downregulated in the epidermis during wound re-epithelialization [10,21]. In wounded mouse dermis, Cx43 abundance is also markedly reduced in hair follicles while it is upregulated in blood vessels [10]. Cx43 is also, in general, upregulated in the dermis in non-healing diabetic human and rat skin wounds compared to non-diabetic wounds [50]. Interestingly, transient blocking of Cx43 expression or function during the early stages of wound healing accelerates wound re-epithelialization and granulation tissue formation in skin in various wound healing models [11,17,18,24,38,39]. In addition, blocking Cx43 function reduces dermal scar formation in rodent models [17,54,63]. In a recent study, immediate or early application of ACT1 (synthetic peptide mimicking the Cx43 C-terminus) gel to human laparoscopic incisional wounds significantly improved scar pigmentation, thickness, and surface roughness as compared to untreated wounds, likely by inhibiting ZO-1 association with endogenous Cx43 [25]. Therefore, early down-regulation of Cx43 function or expression may be beneficial for wound healing and suppress scar formation.

In gingival wound healing, the abundance of Cx43 is strongly reduced in the epithelium and fibroblasts during the early stages of wound healing [69]. Furthermore, selective blockage of Cx43 HCs or GJs by mimetic peptides resulted in a distinct upregulation of anti-fibrotic genes and a downregulation of pro-fibrotic genes in cultured GFBLs, and this response was mainly mediated by Cx43 HCs [70]. Thus, reduced Cx43 HC function may be important for fast and relatively scar-free gingival wound healing. Given that GFBLs and SFBLs have distinct phenotypic properties that may underlie the wound healing outcomes, it is possible that the expression and/or function of Cx43 is also different in these two cell types.

Therefore, the aim of the present studies was to first characterize Cx43 HCs and GJs in human GFBLs and SFBLs *in vivo*. By using a well-established three-dimensional (3D) cell culture model that mimics wound healing [3,31,34,73], we compared the function of Cx43 HCs and GJs in GFBLs and SFBLs. We hypothesized that SFBLs and GFBLs display distinct phenotypes regarding expression and/or function of Cx43, and that this may partly contribute to the different wound healing outcomes in skin and gingiva.

2. Materials and methods

2.1. Human tissue samples

Palatal gingival tissue samples were obtained from three healthy individuals (26-, 27-year-old females and a 48-year-old-male) and processed for frozen sectioning as described previously [69]. Frozen tissue sections from normal human breast (from two 31-year-old female donors) and abdominal (from a 55-year- old male donor) skin of healthy subjects were obtained from Origene Technologies Inc. (Rockville, MD). For the study, a minimum of three tissue sections from each subject was analyzed.

2.2 Pig tissue samples

Skin and palatal gingival tissue samples were obtained from juvenile female red Duroc pigs (Neufeld Farm, Acme, AB, Canada) as described previously [49]. Briefly, three parallel palatal gingival and dorsal skin tissue samples were collected from three pigs, immediately frozen in liquid nitrogen, and used for total RNA isolation and quantitative real-time RT-PCR (qPCR) as described previously [48].

2.3 Cell culture

Human skin fibroblasts (SFBLs; five strains from different donors) from clinically healthy human breast were obtained from PromoCell (Heidelberg, Germany). Human gingival fibroblasts (GFBLs; five strains from different donors) were isolated as previously described [26] from attached gingiva of clinically healthy human donors (Supplemental Table S1). Cells were routinely maintained in Dulbecco's Modified Eagle's medium (DMEM), supplemented with 1% antibiotic/antimycotic and 10% fetal bovine serum (FBS) (Gibco Life Technologies, Inc., Grand Island, NY, USA) at 37 °C and 5% CO_2, and seeded for experiments when they reached about 95% confluence. Experiments were performed at passages 5–10. To generate three-dimensional (3D) *in vivo*-like cultures [3], cells (42,000 cells/cm^2) were seeded and cultured for 24 h, followed by incubation in the above medium supplemented with 50 μg/ml of ascorbic acid up to 14 days, with medium changes every other day [47]. The cultures were serum-starved for 24 h prior to analyses or further treatment (see below).

2.4 Ethics statement

Tissue donors provided written informed consent. All procedures were reviewed and approved by the Office of Research Ethics of the University of British Columbia, and comply with the 1975 Declaration of Helsinki. All animal procedures were reviewed and approved by the Animal Care Committee of the Faculty of Medicine, University of Calgary (Calgary, AB, Canada; protocol number M03037.M08025, 2009).

2.5 Immunostaining

Human frozen tissue sections and fibroblasts grown on gelatin-coated glass coverslips in 24-well plates were fixed and immunostained as described previously [47,69]. Cx43 and Cx43(E2) antibodies were used to localize all Cx43 molecules and Cx43 HCs only, respectively. Antibodies against vimentin and ZO-1 were used to identify fibroblasts and cell-cell contact areas, respectively. All antibodies used are listed in Supplemental Table S2. Images were acquired using optical sectioning at 1 μm (ECLIPSE 80i Microscope; Nikon, Tokyo, Japan), and are presented as z-stacks created by the NIS-Elements BR software (Nikon). Control staining was performed by omitting the primary antibody incubation step. Cx43-positive plaques were quantified from a minimum of 100 cells per culture from five standardized microscopic fields which were derived from three parallel samples using Fiji software [Schindelin et al. [84]; http://fiji.sc/]. The analyses were replicated in two independent experiments. A threshold was set to detect Cx43-positive plaques with minimal background noise, and it remained the same for all images.

2.6 Quantitative real time RT-PCR (qPCR)

qPCR analysis was performed according to MIQE guidelines [6] as we have described in detail previously [69]. The primers used for qPCR and reference genes are listed in Supplemental Table S3. Amplification reactions for qPCR were performed using the CFX96 System (Bio-Rad). For a given experiment, at least two reference genes were chosen [44]. Non-transcribed RNA samples were used as a negative control. The qPCR reactions were performed in triplicate for each sample. The data was analyzed and is presented based on the comparative Ct method (CFX Manager Software Version 2.1, Bio-Rad).

2.7 Western blotting

SFBLs and GFBLs were lysed and collected at indicated time points post-seeding as described previously [47]. Western blotting was performed with the antibody against total Cx43 (Supplemental Table S2). β-Tubulin was used as a loading control. Intensity of the protein bands was quantified using ImageJ software version 1.51 h (NIH, Bethesda, MD; http://imagej.nih.gov/ij).

2.8 Modulation of Cx43 GJ and HC function

GFBLs and SFBLs were grown on 6-well plates as described above. At day-6 post-seeding, cells were serum-starved for 24 h, and then treated with Gap27 (150 μM; SRPTEKTIFII; Biomatik, Cambridge, ON, Canada), which blocks Cx43 GJ and HC functions [8,29,74], or TAT-Gap19 peptide (400 μM; YGRKKRRQRRR-KQIEIKKFK; LifeTein, Somerset, NJ, USA), which specifically blocks Cx43 HCs without affecting GJs [1,75]. Control samples were treated with a scrambled control Gap27 peptide (TFEPDRISITK; Biomatik) [80], or a mutated, function-deficient control TAT-Gap19 peptide (YGRKKRRQRRR-KQAEIKKFK; LeifTein) [74], respectively.

2.9 Dye transfer experiments

Fibroblasts were grown on glass coverslips as described above, and then serum-starved in DMEM for 24 h. To assess the GJ function of Cx43, cells were preincubated with Gap27 (150 μM), TAT-Gap19 (400 μM), or with the corresponding control peptides in DMEM at 37 °C for 1 h. Medium was then removed, cells were scrape-loaded with 0.5% Lucifer Yellow (Molecular Probes Inc., Eugene, OR, USA) for 5 min, and then rinsed and fixed as described previously [69].

To assess the HC function of Cx43, cells were preincubated in their normal growth medium (DMEM; containing 1.8 mM Ca^{2+}), or in EMEM (Lonza, Walkersville, MD, USA) supplemented with 180 nM Ca^{2+} (low calcium medium) to induce the opening of Cx HCs [74], with or without Gap27, TAT-Gap19, or corresponding controls, as above for 1 h. Cultures were then treated in the respective media with the inhibitors or controls, and Propidium Iodide (2.5 mM; Sigma-Aldrich) for 20 min.

2.10 Statistical analysis

The data is presented as mean ± standard error of the mean (s.e.m.) from a minimum of three biological replicates, unless otherwise indicated. Statistical analysis was performed by

using two-tailed *t*-test; $p < 0.05$ was considered statistically significant. Values obtained from the qPCR by the comparative Ct-method were Log2 transformed for statistical testing [58].

3. Results

3.1 Human gingival fibroblasts and epithelial cells show abundant immunostaining of Cx43 HCs compared to skin in vivo

To compare the abundance of Cx43 in skin and gingiva, we first assessed the expression of Cx43 mRNA in paired samples from normal dorsal skin and attached palatal gingiva from three separate red Duroc pigs. The tissue structure and wound healing response in the skin and gingiva of these animals closely resembles that of the corresponding human tissues [16,57,78]. Findings showed that expression of Cx43 mRNA in skin was 4-fold ($p < 0.033$, Student's *t*-test) higher than in gingiva. To investigate the localization of Cx43, tissue sections obtained from human gingiva and skin were immunostained using an antibody that recognizes intracellular, GJ- and HC-associated Cx43 (total Cx43) [64,65], or with an antibody that detects only cell surface HC-associated Cx43 [Cx3(E2); [62,36]]. Consistent with our previous findings [69,70], in gingival epithelium, total Cx43 staining was localized to cell-cell contact areas of keratinocytes, with stronger immunoreactivity at the basal and spinous layers and a less abundant staining at the upper layers (Fig. 1A and B, respectively). In contrast, HC-specific Cx43(E2) staining was present only in the basal and spinous epithelial layers (Fig. 1D), with no immunoreactivity observed at the upper layers (Fig. 1E). Staining of Cx43 plaques with the antibody against total Cx43 detected markedly more plaques in the basal and spinous layers of the epithelium than the Cx43(E2) antibody against Cx43 HCs (Fig. 1A and D, respectively).

Using both antibodies against total Cx43 (Fig. 1C) or Cx43 HCs (Fig. 1F) fairly large plaque-like structures were also detected in GFBLs as identified by double-immunostaining for vimentin. The most notable staining with both Cx43 antibodies was associated with long fibroblast processes (inserts in Fig. 1C and F). Unlike in the epithelium that showed more abundant staining for total Cx43 than Cx43 HCs, the density of the Cx43 plaques stained with both of the antibodies appeared relatively equal in GFBLs.

In dermal epithelium, a very intense immunoreactivity against total Cx43 was observed at the upper layers, with markedly less abundant staining in the basal and spinous layers (Fig. 1G). In contrast to the gingival epithelium, skin epidermis contained few Cx43 HCs located in the superficial layers, while the basal and spinous layers were largely negative (Fig. 1I).

Similar to findings with GFBLs (Fig. 1C and insert), total Cx43-positive plaques were present and located mainly on the long processes of SFBLs (Fig. 1H and insert). However, in contrast to observations with GFBLs (Fig. 1F), Cx43 HC plaques were almost totally absent from SFBLs (Fig. 1J), and when present, were localized along the fibroblast processes as in the GFBLs (insert in Fig. 1J).

Taken together, expression of Cx43 mRNA in skin is significantly higher than in gingiva. In GFBLs *in vivo*, the density of total Cx43 and Cx43 HC plaques are relatively similar,

suggesting that the majority of Cx43 plaques contain Cx43 HCs. In contrast, SFBLs show abundant immunoreactivity for total Cx43, while they possess only very few Cx43 HC plaques. Similarly, skin epidermis shows a stronger total Cx43 staining and fewer Cx43 HC plaques, especially in the basal and spinous layers of the epithelium, compared to the gingival epithelium. In both gingival and skin epithelium, the number of Cx43 positive plaques detected by the total Cx43 antibody is markedly higher than those detected by the HC-specific Cx43(E2) antibody, suggesting that Cx43 HCs comprise a minor proportion of total Cx43 found in both epithelia.

3.2 Skin fibroblasts express increased amount of Cx43 protein but possess fewer Cx43 HCs than gingival fibroblasts in 3D cultures

Having established that SFBLs abundantly display total Cx43-positive plaques but have very few Cx43 HCs compared to GFBLs *in vivo*, we wanted to compare expression and abundance of Cx43 by these cells *in vitro*. To this end, a well-established *in vivo*-like three-dimensional (3D) cell culture model was used. In this model, fibroblasts are initially cultured as a high density monolayer which are then stimulated with serum and ascorbic acid to proliferate, express a transcriptome similar to that observed during wound healing, and produce a multilayered 3D ECM over time, a situation that mimics connective tissue wound healing [3,31,34,73]. In addition, cells become embedded in their own cell type-specific extracellular matrix, allowing them to interact with the 3D matrix using similar cell adhesion receptors found *in vivo* [12,13,23,34,37,56,82]. We have previously shown that GFBLs and SFBLs display distinct tissue-specific phenotypes in this model [47,48]. Using five parallel GFBL and SFBL strains, the expression of key Cxs previously found in fibroblasts (Cx32, Cx37, Cx40, Cx43, and Cx45) were assessed by qPCR. As expected, based on mRNA levels, Cx43 was the major Cx detected in both GFBLs and SFBLs at day-3 post-seeding (Fig. 2A). In addition, both cell types expressed low levels of Cx45, while expression of Cx32, Cx37 and Cx40 was negligible (Fig. 2A). During propagation of the 3D cultures, SFBLs showed a time-dependent and significant increases in Cx43 expression from day-3 to −14 postseeding (Fig. 2B). However, no significant differences were detected in the levels of Cx43 mRNA between GFBLs and SFBLs at any time point studied (Fig. 2A and B). Interestingly, at day-7 post-seeding, when the 3D architecture of the cultures was well established [3,47], SFBLs produced significantly higher levels of Cx43 protein compared to GFBLs (Fig. 2C and D).

To study in more detail the abundance and localization of Cx43 in the 3D cultures, we performed Western blotting for total Cx43 and immunostaining for Cx43 using the antibodies against total and HC-associated Cx43 in GFBLs and SFBLs at 3-, 7- and 14-days post-seeding. Double-immunostaining with ZO-1 was performed to indicate the cell-cell contacts where GJs are formed [71]. Western blotting results showed increasing amount of total Cx43 in both cell types over time (Supplemental Fig. S1). Consistent with our previous findings from GFBLs [70], immunostaining showed few plaques that were positive for total Cx43 antibody and colocalized with ZO-1, likely representing GJ plaques at cell-cell contacts, in both GFBLs and SFBLs (Fig. 2E; a–f). The observation that the majority of the Cx43-positive plaques did not colocalize with ZO-1 suggests that they represented intracellular and/or HC-associated Cx43 (Fig. 2E; a–c). As reported previously for GFBLs

[70], Cx43(E2)-positive HC plaques were present and located throughout the cell body for both GFBLs and SFBLs. As expected, they did not colocalize with ZO-1-positive cell-cell contacts (Fig. 2E; g–l). Quantification of immunostaining indicated that almost equal number of plaques were stained with the antibodies against total Cx43 and Cx43 HCs in GFBLs (Fig. 2F). Thus, in GFBL 3D cultures, most Cx43 assembles into HCs and GFBLs possess only few Cx43 GJs.

When compared to GFBLs, SFBLs displayed somewhat elevated numbers of total Cx43-positive plaques and these differences were most apparent at day-7 and −14 post-seeding (Fig. 2F). However, SFBLs showed markedly fewer Cx43 HCs at day-3 and −7 post-seeding than did GFBLs (Fig. 2F). As a result, the plaques stained with the total Cx43 antibody significantly outnumbered the Cx43 HCs at day-3, −7, and −14 post-seeding in SFBLs (Fig. 2F). Therefore, unlike in GFBLs, only a small proportion of the SFBL Cx43 assembled into HC plaques. The number of these Cx43 HCs in SFBLs increased significantly over time, reaching levels similar to those of GFBLs at day-14 post-seeding (Fig. 2F). Taken together, both GFBLs and SFBLs express Cx43 as their major Cx. In 3D cultures, expression of total Cx43 protein was significantly higher in SFBLs than in GFBLs. Similar to findings in normal skin and gingiva *in vivo*, 3D cultures of SFBLs possessed significantly fewer Cx43 HCs, while they were abundant in GFBLs at day-3 post-seeding. During propagation of the 3D cultures over time, the number of Cx43 HCs in SFBLs increased reaching the levels detected in GFBLs at day-14 post-seeding.

3.3 Gingival and skin fibroblasts possess functional Cx43 GJs and HCs

We have previously shown that cultured GFBLs have functional Cx43 GJs and HCs [69,70]. Having established that SFBLs also possess both Cx43 GJs and HCs, we wanted to also evaluate their functionality. To assess the Cx43 GJ function, GFBLs and SFBLs were cultured for three days as above, scrape-loaded with Lucifer Yellow and dye transfer was followed for 5 min, as described previously [70]. Both GFBLs and SFBLs showed potent dye transfer that extended several cells away from the scratch wound edge indicating that they possess functional GJs (Fig. 3A; a, b, d, e and g, h, j, k, respectively). To confirm whether the dye transfer occurred via Cx43 GJs, cells were pretreated with Gap27, a Cx43 mimetic peptide that binds to the Cx43 extracellular loop and specifically blocks its GJ and HC functions [29,8]. Gap27 treatment effectively blocked dye transfer in both GFBLs and SFBLs indicating that it was mediated by Cx43 (Fig. 3A; c and i, respectively). As expected, treatment of cells with TAT-Gap19 peptide, which specifically blocks Cx43 HC functions without affecting GJs [1,62], did not affect dye transfer in either GFBLs or SFBLs (Fig. 3A; f and i, respectively).

To assess Cx43 HC function, the above cultures were incubated in low Ca^{2+}-containing medium (180 nM Ca^{2+}) to induce the opening of Cx HCs, and then treated with HC-permeable Propidium Iodide (PI) [60]. HC-mediated dye transfer was assessed after 20 min using fluorescence microscopy as described previously [70]. Both GFBLs and SFBLs showed avid PI uptake when kept in low Ca^{2+}-containing medium (Fig. 3B; d and j). As expected, dye transfer was effectively blocked when cells were incubated with high Ca^{2+}-containing medium (1.8 mM Ca^{2+}) (Fig. 3B; a and g) that maintains Cx HCs in a closed

state. Treatment of cells kept in low Ca^{2+}-containing medium with Gap27 (Fig. 3B; e and k) or TAT-Gap19 (Fig. 3B; f and l) resulted in complete blockage of PI uptake as compared to treatments with corresponding control peptides (Fig. 3B; b, h and c, i, respectively). Thus, human GFBLs and SFBLs display functional Cx43 GJs and HCs that can be blocked with Gap27. TAT-Gap19 effectively blocked Cx43 HC function without affecting GJs in both cell types.

3.4 A set of wound healing-associated genes is distinctly regulated via Cx43 GJs and HCs in gingival and skin fibroblasts

Using standard 2D cultures, we have previously shown that Gap27 and TAT-Gap19 significantly regulate expression of a set of wound healing-associated genes in GFBLs, suggesting that Cx43 GJs and HCs play a role in the cell phenotype [69,70]. To explore this further using 3D cultures that better mimic the skin *in vivo*, we next compared gene expression of the previously validated set of wound healing-associated genes [47,69,70] in response to Gap27 and TAT-Gap19 treatment in GFBLs and SFBLs. To this end, cells were maintained in 3D cultures for seven days, treated with Gap27 (150 μM) to block both Cx43 GJs and HCs or TAT-Gap19 (400 μM) to block Cx43 HCs only for 24 h, and gene expression assessed by qPCR. At this time point, SFBLs expressed significantly higher levels of Cx43 proteins, but had a markedly lower abundance of Cx43 HCs than GFBLs (Fig. 2C–F). Results showed that compared to controls, both Gap27 and TAT-Gap19 treatments significantly increased the expression of 10 of the 25 genes analyzed in GFBLs (MMP-1, −3, −10, TIMP-1, Tenascin-C, TGF-β1, TGF- β3, VEGF-A, Cx43, and Cadherin-2). The expression of seven of these 10 genes (MMP-1, −3, −10, Tenascin-C, VEGF-A, Cx43, and Cadherin-2) was significantly more potently upregulated by TAT-Gap19 compared to Gap27 treatment (Fig. 4A). Five other genes (TIMP-3, Collagen type I, NMMIIB, NAB1, and CXCL12) were significantly regulated only by TAT-Gap19 (Fig. 4A). In contrast, two genes (TIMP-4 and Collagen type III) were significantly regulated only by Gap27 treatment. Neither of the peptide treatments had a significant effect on eight of the genes assessed (MMP-14, TIMP-2, EDA-FN, EDB-FN, α-SMA, Decorin, Fibromodulin, and Cx45) (Fig. 4A).

When compared to controls, only four (MMP-1, −3, −10, and VEGF-A) out of the above 25 genes were significantly increased by both Gap27 and TAT-Gap19 treatments in SFBLs (Fig. 4B). Further analysis showed that eight of the studied genes (TIMP-3, Collagen type I, EDA-FN, EDB-FN, NMMIIB, Decorin, Fibromodulin, and CXCL12) showed a different response to the two peptide treatments in SFBLs (Fig. 4B). Among these genes, EDB-FN was significantly upregulated only by the Gap27 treatment. Out of the remaining seven genes, two (TIMP-3 and EDA-FN) were significantly upregulated, and five (Collagen type I, NMMIIB, Decorin, Fibromodulin, and CXCL12) were downregulated by TAT-Gap19, while Gap27 had no effect (Fig. 4B). Out of the 25 genes analyzed, 13 genes (MMP-14, TIMP-1, −2, −4, Collagen type III, Tenascin-C, α-SMA, TGF-β1, TGF-β3, NAB1, Cx43, Cx45, and Cadherin-2) did not show significant expression changes in response to either of the peptide treatments in SFBLs (Fig. 4B). This indicates that expression of these genes is not under the control of Cx43 GJs or HCs in SFBLs in this model. Findings from a set of additional experiments showed that for the genes that responded to the Gap27 and TAT-Gap19

treatments, the responses were concentration-dependent from 50 μM up to 300 μM, and from 400 μM up to 600 μM, respectively (Supplemental Fig. S2). Therefore, the expression of a set of wound healing-related genes is distinctly regulated by Gap27 and TAT-Gap19 in GFBLs and SFBLs (Fig. 4 and Table 1).

3.5. Gap27 and TAT-Gap19 treatments distinctly modulate expression of a set of wound healing-associated genes in human gingival compared to skin fibroblasts

Next, we wanted to evaluate the effect of each peptide treatment on GFBLs and SFBLs to compare the response patterns. To this end, we compared the gene expression changes induced by Gap27 (Fig. 5A) or TAT-Gap19 (Fig. 5B) relative to corresponding control peptide-treated samples between GFBLs and SFBLs. MMP3 was the only gene that was significantly upregulated by TAT-Gap19 in both GFBLs and SFBLs (Fig. 4A and B), and which showed a significantly more pronounced upregulation in GFBLs compared to SFBLs (Fig. 5B). Out of the remaining 24 genes studied, expression of three genes (TGF-β1, TGF-β3, and Cx43) was significantly higher after treatment with both Gap27 (Fig. 5A) and TAT-Gap19 (Fig. 5B) in GFBLs compared to SFBLs, as only GFBLs responded to the treatments. Likewise, two genes (TIMP-1 and Cadherin-2) showed increased expression in response to TAT-Gap19 treatment in GFBLs, but not in SFBLs (Fig. 5B). Decorin was significantly downregulated in SFBLs compared to GFBLs by TAT-Gap19 because only SFBLs responded to the treatment (Fig. 5A). Thus, the expression of the above seven genes (MMP-3, TIMP-1, TGF-β1, TGF- β3, Cx43, Decorin, and Cadherin-2) was significantly influenced by TAT-Gap19 in GFBLs compared to SFBLs. Three of the above seven genes (TGF- β1, TGF- β3, and Cx43) were also potently regulated by Gap27 in GFBLs, but not in SFBLs. Therefore, the phenotype of GFBLs was more potently regulated by Gap27 and TAT-Gap19 than SFBLs.

4. Discussion

GFBLs and SFBLs from normal tissue display distinct phenotypes, and this may contribute to the different wound healing outcomes in these two tissues [19,47–49,78]. The expression and function of Cx43 is also an important modulator of wound healing [9]. We have shown that in human gingiva, fibroblasts and keratinocytes assemble Cx43 into both GJ and HC plaques *in vivo* [69,70]. Findings from other human studies have also shown the presence of Cx43 GJs in skin keratinocytes *in vivo* [4]. However, it is not known whether these two tissues distinctly express Cx43 GJs and HCs. Findings from the present studies demonstrated that, similar to the gingival tissue [70], Cx43 assembles into GJ and HC plaques in human skin epithelium and connective tissue fibroblasts *in vivo*. However, gingiva and skin showed marked differences in the abundance of Cx43. Based on analysis of pig tissue samples that contained both epithelium and connective tissue, skin expressed significantly higher levels of Cx43 mRNA than did gingiva. Cx43 immunostaining was also greater in the human skin epidermis compared to gingival epithelium. More specifically, in skin epidermis total Cx43-positive plaques were most abundant at the upper epidermal layers with notably less staining in the basal and spinous layers, which is consistent with previous findings [4]. Cx43(E2) staining, on the other hand, showed very few and weakly positive Cx43 HC plaques at the spinous and upper epithelial layers, while the basal layer

was negative. Therefore, in the skin epidermis, Cx43 forms mainly GJ plaques and only few HCs are present and localize to the suprabasal layers. In contrast to the epidermis, in gingival epithelium, Cx43 was assembled into distinct GJ and HC plaques at the basal and spinous layers. However, the upper keratinocytes presented only Cx43-positive GJs and no HCs. Thus, human skin epithelium possesses markedly greater abundance of total Cx43-positive plaques, but few Cx43 HCs as compared to gingival epithelium. The different localization of total Cx43 and Cx43 HCs into basal and suprabasal layers in gingival and skin epithelium, respectively, suggests that Cx43 plays distinct roles in keratinocyte differentiation and function in these two tissues. Cx43 expression and GJ formation modulates keratinocyte differentiation in organotypic cultures and during fetal development [2,40,77], but the role of Cx43 HCs in this process and in other keratinocyte functions is poorly understood.

In connective tissue, Cx43 was also present in SFBLs and GFBLs *in vivo*, with Cx43-positive plaques localized on the cell body and processes. Interestingly, however, Cx43 HCs were almost totally absent in SFBLs, while in GFBLs their abundance appeared similar to the plaques stained with the total Cx43 antibody. Therefore, GFBLs appear to mainly contain Cx43 HCs, while in SFBLs Cx43 plaques may represent mostly GJs *in vivo*. Findings from dye transfer experiments have shown that fibroblasts residing in intact human skin likely communicate with each other through the GJs although the identity of the Cxs involved remained unknown [59]. As Cx43 is the major Cx in SFBLs and GFBLs, it is likely that it also plays a key role in gap junctional intercellular communication (GJIC) in these tissues *in vivo*. In any case, it is intriguing that SFBLs largely lacked Cx43 HCs while they were abundant in GFBLs *in vivo*. Clearly, the functional role of Cx43 HCs in skin and gingival connective tissue, like in the epithelium, needs further clarification. The functional significance of the higher abundance of Cx43 HCs in normal gingival epithelium and fibroblasts as compared to skin may relate to the relatively high tissue turnover rate in gingival epithelium and connective tissue compared to skin [19]. In addition, unlike skin, healthy gingiva is characterized by a subclinical inflammation [7] that may be important for the defense against oral microbes. It is well established that Cx43 HCs play a key role in the inflammatory response [76], but their role in gingiva has remained unexplored.

In any case, there is strong evidence that Cx43 plays an important role in wound healing [45,54] and distinct expression or function of Cx43 in gingiva and skin may contribute to different wound healing outcomes in these tissues. Our previous findings have shown that while the abundance of total Cx43 is strongly downregulated in GFBLs during the early inflammatory and granulation tissue formation stages of gingival wound healing, there is a gradual increase in Cx43 abundance during the matrix deposition and remodeling stages of healing [69]. Furthermore, a transient downregulation of Cx43 expression or function at the early stages of wound healing promotes skin wound closure and reduces scaring [45,54]. Therefore, to compare Cx43 expression and function in GFBLs and SFBLs in relation to wound healing, we used five cell lines of human GFBLs and SFBLs in a 3D culture model, which mimics the matrix deposition and remodeling stages of wound healing better than the traditional 2D cultures [12,13,23,31,34,56,73]. In this model, Cx43 was the major Cx expressed by both GFBLs and SFBLs, and it formed functional GJs and HCs in both cell types. While GFBLs and SFBLs did not show significant differences in Cx43 mRNA

expression, SFBLs produced significantly higher levels of total Cx43 protein. This suggests that posttranscriptional Cx43 processing and turnover is distinctly regulated in SFBLs and GFBLs. In many cell types, Cx43 turnover is fast, and involves several mechanisms that modulate its biosynthesis, transport and assembly in the cell membrane, endocytosis, degradation and recycling [52]. Very little is known about these processes specifically in fibroblasts. Nonetheless, based on immunostaining with total and Cx43 HC-specific antibodies, and consistent with our previous data from standard 2D cultures [70], Cx43 was mainly assembled into HC plaques in GFBLs. Interestingly, in day-3 and −7 cultures, SFBLs displayed significantly less Cx43 HCs than did GFBLs, which is similar to the above findings *in vivo*. The abundance of Cx43 HCs in SFBLs increased over time, reaching levels similar to those of GFBLs by day-14 post-seeding. Collectively, in this model, SFBLs, but not GFBLs, increase the abundance and distribution of Cx43 into HC plaques over time. In order to explore the functional significance of this finding, we used Cx43 mimetic peptides as tools to dissect regulation of gene expression by Cx43 GJs and HCs in SFBLs compared to GFBLs. Gap27 blocks both of its GJ and HC functions [29,8], while TAT-Gap19 blocks only Cx43 HC functions without affecting GJs [74]. In addition, TAT-Gap19 may also affect Cx43 channel-independent functions by inducing conformational changes that perturb interactions of the cytoplasmic domains with intracellular signaling molecules [1,30,51,74]. Our analysis focused on 21 wound healing-related genes that were previously regulated by these peptides in standard 2D cultures of GFBLs. We also included four genes in the analysis that were not regulated by either of the peptides in 2D cultures of GFBLs [69,70]. Similar to the 2D cultures [69,70], the above four genes were not regulated by either of peptide treatments in GFBLs also in this 3D model. As in our previous study of GFBLs in 2D cultures, the expression of nine genes was regulated by only Gap27 treatment or by both peptides, respectively, also in the 3D model. The expression of the remaining eight genes, however, was apparently regulated by different mechanisms in the 3D model when compared to the previous 2D model data (Supplemental Table S4) [70]. Taken together, the function of Cx43 GJs and HCs in GFBLs may be modulated by the 3D environment distinctly from the 2D cultures. Cx GJIC and HC functions and signaling can be regulated by various mechanisms that involve interplay with signals elicited by cell adhesion to the extracellular matrix, mechanosensing, and auto- and paracrine cytokines/growth factors, which may be different between the 2D and 3D cultures [13,34,71,79,82].

When comparing gene expression changes induced by the peptide treatments between GFBLs and SFBLs in the 3D model, 12 out of 25 studied genes showed similar responses to the peptide treatments in both GFBLs and SFBLs. From these genes, the expression of MMP-14, TIMP-2, α-SMA, and Cx45 was not regulated by either of the peptides in both cell types, suggesting that their expression is not regulated by Cx43 in either GFBLs or SFBLs. Interestingly, 13 genes were differently regulated by the peptide treatments in GFBLs and SFBLs. These genes included six ECM proteins (EDA-FN, EDB-FN, Collagen type III, Tenascin-C, Decorin, and Fibromodulin) involved in wound healing [27], two protease inhibitors (TIMP-1 and TIMP-4) that modulate inflammation and tissue remodeling [15,66], and three TGF-β signaling-related genes (TGF-β1, TGF-β3, and NAB1) involved in fibrosis and scar formation [55]. They also included Cx43 and Cadherin-2, which play a role in intercellular communications [14]. From the above 13 genes, six (TIMP-1, Tenascin-C,

TGF-β1, TGF- β3, Cx43, and Cadherin-2) were significantly upregulated by both Gap27 and TAT-Gap19 treatments in GFBLs, suggesting that they are regulated by Cx43 HCs in these cells. In contrast, expression of these six genes was not affected by either of the peptide treatments in SFBLs. Moreover, the expression of EDB-FN in SFBLs and TIMP-4 and Collagen type III in GFBLs was regulated by only Gap27 and not by TAT-Gap19, suggesting that these genes are distinctly regulated by Cx43 GJs in GFBLs and SFBLs.

It is intriguing that some genes in both GFBLs and SFBLs (TIMP-3, Collagen Type I, NMMBII, and CXCL12), or in only GFBLs (NAB1) or SFBLs (EDA-FN, Decorin, and Fibromodulin) were significantly regulated by TAT-Gap19 but not with Gap27, although both peptides are expected to block Cx43 HCs. Gap27 binds to the Cx43 extracellular loop, whereas TAT-Gap19 binds to the L2 domain of the cytoplasmic loop altering its interaction with the C-terminal tail. In addition to blocking Cx43 HC functions, this may perturb interactions of the Cx43 cytoplasmic domains with the intracellular signaling molecules affecting Cx43 channel-independent signaling [1,30,51,74]. Therefore, it is possible that the expression changes in the above genes resulting from exposure to only TAT-Gap19 are mediated by the channel-independent functions of Cx43. Distinct regulation of the above four genes (NAB1, EDA-FN, Decorin, and Fibromodulin) by this mechanism in GFBLs compared to SFBLs suggests that Cx43 channel-independent functions are also distinctly regulated in these two cell types in this model.

To summarize, we have shown for the first time that Cx43 distinctly assembles into Cx43 GJs and HCs in human skin and gingiva *in vivo*. Interestingly, in contrast to GFBLs, Cx43 HCs composed only a small proportion of total Cx43 in SFBLs *in vivo* and *in vitro*. Using the 3D culture model, we further showed that the GJ, HC, and channel-independent functions of Cx43, the major Cx expressed by these cells, distinctly regulate wound healing-related gene expression patterns in GFBLs and SFBLs. Therefore, it is possible that the distinct wound healing outcomes in skin and gingiva may partly derive from inherently different assembly and function of Cx43 in the resident fibroblasts.

Supplementary Material

Refer to Web version on PubMed Central for supplementary material.

Acknowledgments

This work was supported by Canadian Institutes of Health Research (MOP-77550 and PJT-153223 to LH), Natural Sciences and Engineering Research Council of Canada (RGPIN-2017–05765 LH), National Institute of Health (CA196214 to JXJ), Welch Foundation Grant (AQ-1507 to JXJ), and UBC Faculty of Dentistry Graduate Awards (RT).

Abbreviations:

GFBLs	Gingival fibroblasts
SFBLs	Skin fibroblasts

References

[1]. Abudara V, Bechberger J, Freitas-Andrade M, De Bock M, Wang N, Bultynck G, Naus CC, Leybaert L, Giaume C, The connexin43 mimetic peptide Gap19 inhibits hemichannels without altering gap junctional communication in astrocytes, Front. Cell Neurosci. 21 (2014) 306.

[2]. Arita K, Akiyama M, Tsuji Y, McMillan JR, Eady RA, Shimizu H, Changes in gap junction distribution and connexin expression pattern during human fetal skin development, J. Histochem. Cytochem 50 (2002) 1493–1500. [PubMed: 12417615]

[3]. Beacham DA, Amatangelo MD, Cukierman E, Preparation of extracellular matrices produced by cultured and primary fibroblasts, Curr. Protoc. Cell Biol (2007) (Chapter 10:Unit 10.9).

[4]. Brandner JM, Houdek P, Hüsing B, Kaiser C, Moll I, Connexin 26, 30, and 43: differences among spontaneous, chronic, and accelerated human wound healing, J. Investig. Dermatol 122 (2004) 1310–1320. [PubMed: 15140236]

[5]. Burra S, Jiang JX, Regulation of cellular function by connexin hemichannels, Int. J. Biochem. Mol. Biol 2 (2011) 119–128.

[6]. Bustin SA, Benes V, Garson JA, Hellemans J, Huggett J, Kubista M, Mueller R, Nolan T, Pfaffl MW, Shipley GL, Vandesompele J, Wittwer CT, The MIQE guidelines: minimum information for publication of quantitative real-time PCR experiments, Clin. Chem 55 (2009) 611–622. [PubMed: 19246619]

[7]. Cekici A, Kantarci A, Hasturk H, Van Dyke TE, Inflammatory and immune pathways in the pathogenesis of periodontal disease, Periodontol 2000 (64) (2014) 57–80.

[8]. Chaytor AT, Evans WH, Griffith TM, Peptides homologous to extracellular loop motifs of connexin 43 reversibly abolish rhythmic contractile activity in rabbit arteries, J. Physiol 503 (1997) 99–110. [PubMed: 9288678]

[9]. Cogliati B, Mennecier G, Willebrords J, Da Silva TC, Maes M, Pereira IVA, Crespo-Yanguas S, Hernandez-Blazquez FJ, Dagli MLZ, Vinken M, Connexins, pannexins, and their channels in fibroproliferative diseases, J. Membr. Biol 249 (2016) 199–213. [PubMed: 26914707]

[10]. Coutinho P, Qiu C, Frank S, Tamber K, Becker D, Dynamic changes in connexin expression correlate with key events in the wound healing process, Cell Biol. Int 27 (2003) 525–541. [PubMed: 12842092]

[11]. Coutinho P, Qiu C, Frank S, Wang CM, Brown T, Green CR, Becker DL, Limiting burn extension by transient inhibition of Connexin43 expression at the site of injury, Br. J. Plast. Surg 58 (2005) 658–667. [PubMed: 15927148]

[12]. Cukierman E, Pankov R, Stevens DR, Yamada KM, Taking cell-matrix adhesions to the third dimension, Science 294 (2001) 1708–1712. [PubMed: 11721053]

[13]. Cukierman E, Pankov R, Yamada KM, Cell interactions with three-dimensional matrices, Curr. Opin. Cell Biol 14 (2002) 633–639. [PubMed: 12231360]

[14]. Dbouk HA, Mroue RM, El-Sabban ME, Talhouk RS, Connexins: a myriad of functions extending beyond assembly of gap junction channels, Cell Commun. Signal 12 (7) (2009) 4.

[15]. Dufour A, Overall CM, Missing the target: matrix metalloproteinase antitargets in inflammation and cancer, Trends Pharmacol. Sci 34 (2013) 233–242. [PubMed: 23541335]

[16]. Gallant-Behm CL, Olson ME, Hart DA, Cytokine and growth factor mRNA expression patterns associated with the hypercontracted, hyperpigmented healing phenotype of red duroc pigs: a model of abnormal human scar development? J. Cutan. Med Surg 9 (2005) (165e177).

[17]. Ghatnekar GS, O'Quinn MP, Jourdan LJ, Gurjarpadhye AA, Draughn RL, Gourdie RG, Connexin43 carboxyl-terminal peptides reduce scar progenitor and promote regenerative healing following skin wounding, Regen. Med 4 (2009) 205–223. [PubMed: 19317641]

[18]. Ghatnekar GS, Grek CL, Armstrong DG, Desai SC, Gourdie RG, The effect of a connexin43-based Peptide on the healing of chronic venous leg ulcers: a multicenter, randomized trial, J. Investig. Dermatol 135 (2015) 289–298. [PubMed: 25072595]

[19]. Glim JE, van Egmond M, Niessen FB, Everts V, Beelen RH, Detrimental dermal wound healing: what can we learn from the oral mucosa? Wound Repair Regen 21 (2013) 648–660. [PubMed: 23927738]

[20]. Glim JE, Everts V, Niessen FB, Ulrich MM, Beelen RH, Extracellular matrix components of oral mucosa differ from skin and resemble that of fetal skin, Arch. Oral Biol 59 (2014) (1048e1055).

[21]. Goliger JA, Paul DL, Wounding alters epidermal connexin expression and gap junction-mediated intercellular communication, Mol. Biol. Cell 6 (1995) 1491–1501. [PubMed: 8589451]

[22]. Greaves NS, Ashcroft KJ, Baguneid M, Bayat A, Current understanding of molecular and cellular mechanisms in fibroplasia and angiogenesis during acute wound healing, J. Dermatol. Sci 72 (2013) (206e217).

[23]. Green JA, Yamada KM, Three-dimensional microenvironments modulate fibroblast signaling responses, Adv. Drug Deliv. Rev 59 (2007) 1293–1298. [PubMed: 17825946]

[24]. Grek CL, Prasad GM, Viswanathan V, Armstrong DG, Gourdie RG, Ghatnekar GS, Topical administration of a connexin43-based peptide augments healing of chronic neuropathic diabetic foot ulcers. A multicenter, randomized trial, Wound Repair Regen 23 (2015) 203–212. [PubMed: 25703647]

[25]. Grek CL, Montgomery J, Sharma M, Ravi A, Rajkumar JS, Moyer KE, Gourdie RG, Ghatnekar GS, A multicenter randomized controlled trial evaluating a Cx43-mimetic peptide in cutaneous scarring, J. Investig. Dermatol 137 (2017) 620–630. [PubMed: 27856288]

[26]. Häkkinen L, Heino J, Koivisto L, Larjava H, Altered interaction of human granulation-tissue fibroblasts with fibronectin is regulated by alpha 5 beta 1 integrin, Biochim. Biophys. Acta 1224 (1994) 33–42. [PubMed: 7524685]

[27]. Häkkinen L, Larjava H, Koivisto L, Granulation tissue formation and remodeling, in: Larjava H (Ed.), Oral Wound Healing: Cell Biology and Clinical Management, John Wiley & Sons, Inc, Ames, USA, 2012, pp. 125–173.

[28]. Häkkinen L, Larjava H, Fournier BPJ, Distinct phenotype and therapeutic potential of gingival fibroblasts, Cytotherapy 16 (2014) 1171–1186. [PubMed: 24934304]

[29]. Hawat G, Hélie P, Baroudi G, Single intravenous low-dose injections of connexin 43 mimetic peptides protect ischemic heart in vivo against myocardial infarction, J. Mol. Cell Cardiol 53 (2012) 559–566. [PubMed: 22841862]

[30]. Hervé JC, Derangeon M, Sarrouilhe D, Giepmans BN, Bourmeyster N, Gap junctional channels are parts of multiprotein complexes, Biochim. Biophys. Acta 1818 (2012) 1844–1865. [PubMed: 22197781]

[31]. Iyer VR, Eisen MB, Ross DT, Schuler G, Moore T, Lee JC, Trent JM, Staudt LM, Hudson J, Jr, Boguski MS, Lashkari D, Shalon D, Botstein D, Brown PO, The transcriptional program in the response of human fibroblasts to serum, Science 283 (1999) (83e87).

[32]. Iyyathurai J, D'hondt C, Wang N, De Bock M, Himpens B, Retamal MA, Stehberg J, Leybaert L, Bultynck G, Peptides and peptide-derived molecules targeting the intracellular domains of Cx43: gap junctions versus hemichannels, Neuropharmacology 75 (2013) 491–505. [PubMed: 23664811]

[33]. Jiang JX, Gu S, Gap junction- and hemichannel-independent actions of connexins, Biochim. Biophys. Acta 1711 (2005) 208–214. [PubMed: 15955305]

[34]. Kaukonen R, Jacquemet G, Hamidi H, Ivaska J, Cell-derived matrices for studying cell proliferation and directional migration in a complex 3D microenvironment, Nat. Protoc 12 (2017) 2376–2390. [PubMed: 29048422]

[35]. Kar R, Batra N, Riquelme MA, Jiang JX, Biological role of connexin intercellular channels and hemichannels, Arch. Biochem. Biophys 524 (2012) 2–15. [PubMed: 22430362]

[36]. Kar R, Riquelme MA, Werner S, Jiang JX, Connexin 43 channels protect osteocytes against oxidative stress-induced cell death, J. Bone Miner. Res 28 (2013) 1611–1621. [PubMed: 23456878]

[37]. Kimlin LC, Casagrande G, Virador VM, In vitro three-dimensional (3D) models in cancer research: an update, Mol. Carcinog 52 (2013) 167–182. [PubMed: 22162252]

[38]. Kretz M, Euwens C, Hombach S, Eckardt D, Teubner B, Traub O, Willecke K, Ott T, Altered connexin expression and wound healing in the epidermis of connexin-deficient mice, J. Cell Sci 116 (2003) 3443–3452. [PubMed: 12840073]

[39]. Kretz M, Maass K, Willecke K, Expression and function of connexins in the epidermis, analyzed with transgenic mouse mutants, Eur. J. Cell Biol 83 (2004) 647–654. [PubMed: 15679109]

[40]. Langlois S, Maher AC, Manias JL, Shao Q, Kidder GM, Laird DW, Connexin levels regulate keratinocyte differentiation in the epidermis, J. Biol. Chem 282 (2007) 30171–30180. [PubMed: 17693411]

[41]. Lauf U, Giepmans B, Lopez P, Braconnot S, Chen SC, Falk MM, Dynamic trafficking and delivery of connexons to the plasma membrane and accretion to gap junctions in living cells, Proc. Natl. Acad. Sci. USA 99 (2002) 10446–10451. [PubMed: 12149451]

[42]. Larjava H, Wiebe C, Gallant-Behm C, Hart DA, Heino J, Häkkinen L, Exploring scarless healing of oral soft tissues, J. Can. Dent. Assoc 77 (2011) b18. [PubMed: 21366956]

[43]. Leavitt T, Hu MS, Marshall CD, Barnes LA, Lorenz HP, Longaker MT, Scarless wound healing: finding the right cells and signals, Cell Tissue Res 365 (2016) 483–493. [PubMed: 27256396]

[44]. Liu LL, Zhao H, Ma TF, Ge F, Chen CS, Zhang YP, Identification of valid reference genes for the normalization of RT-qPCR expression studies in human breast cancer cell lines treated with and without transient transfection, PLoS One 10 (2015) e0117058. [PubMed: 25617865]

[45]. Lorraine C, Wright CS, Martin PE, Connexin43 plays diverse roles in co-ordinating cell migration and wound closure events, Biochem. Soc. Trans 43 (2015) 482–488. [PubMed: 26009195]

[46]. Lorimier S, Hornebeck W, Godeau G, Pellat B, Gillery P, Maquart FX, Laurent-Maquin D, Morphometric studies of collagen and fibrin lattices contracted by human gingival fibroblasts; comparison with dermal fibroblasts, J. Dent. Res 77 (1998) (1717e29).

[47]. Mah W, Jiang G, Olver D, Cheung G, Kim B, Larjava H, Häkkinen L, Human gingival fibroblasts display a non-fibrotic phenotype distinct from skin fibroblasts in three-dimensional cultures, PLoS One 9 (2014) e90715. [PubMed: 24608113]

[48]. Mah W, Jiang G, Olver D, Gallant-Behm C, Wiebe C, Hart DA, Koivisto L, Larjava H, Häkkinen L, Elevated CD26 expression by skin fibroblasts distinguishes a profibrotic phenotype involved in scar formation compared to gingival fibroblasts, Am. J. Pathol 187 (2017) 1717–1735. [PubMed: 28641076]

[49]. Mak K, Manji A, Gallant-Behm C, Wiebe C, Hart DA, Larjava H, Häkkinen L, Scarless healing of oral mucosa is characterized by faster resolution of inflammation and control of myofibroblast action compared to skin wounds in the red Duroc pig model, J. Dermatol. Sci 56 (2009) 168–180. [PubMed: 19854029]

[50]. Mendoza-Naranjo A, Cormie P, Serrano AE, Wang CM, Thrasivoulou C, Sutcliffe JE, Gilmartin DJ, Tsui J, Serena TE, Phillips AR, Becker DL, Overexpression of the gap junction protein Cx43 as found in diabetic foot ulcers can retard fibroblast migration, Cell Biol. Int 36 (2012) 661–667. [PubMed: 22455314]

[51]. Nambara C, Kawasaki Y, Yamasaki H, Role of the cytoplasmic loop domain of Cx43 in its intracellular localization and function: possible interaction with cadherin, J. Membr. Biol 217 (2007) 63–69. [PubMed: 17627324]

[52]. Nielsen MS, Axelsen LN, Sorgen PL, Verma V, Delmar M, Holstein- Rathlou NH, Gap junctions, Compr. Physiol 2 (2012) 1981–2035. [PubMed: 23723031]

[53]. Nishi H, Ohta K, Takechi M, Yoneda S, Hiraoka M, Kamata N, Wound healing effects of gingival fibroblasts cultured in animal-free medium, Oral Dis 16 (2010) 438–444. [PubMed: 20233319]

[54]. Ongstad EL, O'Quinn MP, Ghatnekar GS, Yost MJ, Gourdie RG, A Connexin43 mimetic peptide promotes regenerative healing and improves mechanical properties in skin and heart, Adv. Wound Care 2 (2013) 55–62.

[55]. Penn JW, Grobbelaar AO, Rolfe KJ, The role of the TGF-β family in wound healing, burns and scarring: a review, Int. J. Burns Trauma 2 (2012) 18–28. [PubMed: 22928164]

[56]. Pouyani T, Papp S, Schaffer L, Tissue-engineered fetal dermal matrices, In Vitro Cell Dev. Biol. Anim 48 (2012) 493–506. [PubMed: 22956043]

[57]. Ramos ML, Gragnani A, Ferreira LM, Is there an ideal animal model to study hypertrophic scarring? J. Burn Care Res 29 (2008) 363–368. [PubMed: 18354295]

[58]. Rieu I, Powers SJ, Real-time quantitative RT-PCR: design, calculations, and statistics, Plant Cell 21 (2009) 1031–1033. [PubMed: 19395682]

[59]. Salomon D, Saurat JH, Meda P, Cell-to-cell communication within intact human skin, J. Clin. Investig 82 (1988) 248–254. [PubMed: 2455735]

[60]. Schalper KA, Palacios-Prado N, Orellana JA, Sáez JC, Currently used methods for identification and characterization of hemichannels, Cell Commun. Adhes 15 (2008) 207–218. [PubMed: 18649191]

[61]. Schalper KA, Riquelme MA, Brañes MC, Martinez AD, Vega JL, Berthoud VM, Bennett MV, Saez JC, Modulation of gap junction channels and hemichannels by growth factors, Mol. Biosyst 8 (2012) 685–698. [PubMed: 22218428]

[62]. Siller-Jackson AJ, Burra S, Gu S, Xia X, Bonewald LF, Sprague E, Jiang JX, Adaptation of connexin 43-hemichannel prostaglandin release to mechanical loading, J. Biol. Chem 283 (2008) 26374–26382. [PubMed: 18676366]

[63]. Soder BL, Propst JT, Brooks TM, Goodwin RL, Friedman HI, Yost MJ, Gourdie RG, The connexin43carboxyl-terminal peptide ACT1 modulates the biological response to silicone implants, Plast. Reconstr. Surg 123 (2009) 1440–1451. [PubMed: 19407614]

[64]. Solan JL, Lampe PD, Connexin43 phosphorylation: structural changes and biological effects, Biochem. J 419 (2009) 261–272. [PubMed: 19309313]

[65]. Sosinsky GE, Solan JL, Gaietta GM, Ngan L, Lee GJ, Mackey MR, Lampe PD, The C-terminus of connexin43 adopts different conformations in the Golgi and gap junction as detected with structure-specific antibodies, Biochem. J 408 (2007) 375–385. [PubMed: 17714073]

[66]. Steffensen B, Häkkinen L, Larjava H, Proteolytic events of wound-healing–coordinated interactions among matrix metalloproteinases (MMPs), integrins, and extracellular matrix molecules, Crit. Rev. Oral Biol. Med 12 (2001) 373–398. [PubMed: 12002821]

[67]. Sutcliffe JE, Chin KY, Thrasivoulou C, Serena TE, O'Neil S, Hu R, White AM, Madden L, Richards T, Phillips AR, Becker DL, Abnormal connexin expression in human chronic wounds, Br. J. Dermatol 173 (2015) 1205–1215. [PubMed: 26264563]

[68]. Szpaderska AM, Zuckerman JD, DiPietro LA, Differential injury responses in oral mucosal and cutaneous wounds, J. Dent. Res 82 (2003) 621–626. [PubMed: 12885847]

[69]. Tarzemany R, Jiang G, Larjava H, Häkkinen L, Expression and function of connexin 43 in human gingival wound healing and fibroblasts, PLoS One 10 (1) (2015) e0115524. [PubMed: 25584940]

[70]. Tarzemany R, Jiang G, Jiang JX, Larjava H, Häkkinen L, Connexin 43 hemichannels regulate the expression of wound healing-associated genes in human gingival fibroblasts, Sci. Rep 7 (2017) 14157. [PubMed: 29074845]

[71]. Thévenin AF, Kowal TJ, Fong JT, Kells RM, Fisher CG, Falk MM, Proteins and mechanisms regulating gap-junction assembly, internalization, and degradation, Physiology 28 (2013) 93–116. [PubMed: 23455769]

[72]. Thulabandu V, Chen D, Atit RP, Dermal fibroblast in cutaneous development and healing, Wiley Interdiscip. Rev. Dev. Biol 7 (2) (2018).

[73]. Walmsley GG, Rinkevich Y, Hu MS, Montoro DT, Lo DD, McArdle A, Maan ZN, Morrison SD, Duscher D, Whittam AJ, Wong VW, Weissman IL, Gurtner GC, Longaker MT, Live fibroblast harvest reveals surface marker shift in vitro, Tissue Eng. Part C Methods 21 (2015) 314–321. [PubMed: 25275778]

[74]. Wang N, De Vuyst E, Ponsaerts R, Boengler K, Palacios-Prado N, Wauman J, Lai CP, De Bock M, Decrock E, Bol M, Vinken M, Rogiers V, Tavernier J, Evans WH, Naus CC, Bukauskas FF, Sipido KR, Heusch G, Schulz R, Bultynck G, Leybaert L, Selective inhibition of Cx43 hemichannels by Gap19 and its impact on myocardial ischemia/reperfusion injury, Basic Res. Cardiol 108 (2013) 309. [PubMed: 23184389]

[75]. Wang N, De Bock M, Decrock E, Bol M, Gadicherla A, Bultynck G, Leybaert L, Connexin targeting peptides as inhibitors of voltage- and intracellular Ca2+ -triggered Cx43 hemichannel opening, Neuropharmacology 75 (2013) 506–516. [PubMed: 24007825]

[76]. Willebrords J, Crespo Yanguas S, Maes M, Decrock E, Wang N, Leybaert L, Kwak BR, Green CR, Cogliati B, Vinken M, Connexins and their channels in inflammation, Crit. Rev. Biochem. Mol. Biol 51 (2016) 413–439. [PubMed: 27387655]

[77]. Wiszniewski L, Limat A, Saurat JH, Meda P, Salomon D, Differential expression of connexins during stratification of human keratinocytes, J. Investig. Dermatol 115 (2000) 278–285. [PubMed: 10951247]

[78]. Wong JW, Gallant-Behm C, Wiebe C, Mak K, Hart DA, Larjava H, Häkkinen L, Wound healing in oral mucosa results in reduced scar formation as compared with skin: evidence from the red Duroc pig model and humans, Wound Repair Regen 17 (2009) 717–729. [PubMed: 19769724]

[79]. Wong P, Laxton V, Srivastava S, Chan YW, Tse G, The role of gap junctions in inflammatory and neoplastic disorders (Review), Int. J. Mol. Med 39 (2017) 498–506. [PubMed: 28098880]

[80]. Wright CS, Pollok S, Flint DJ, Brandner JM, Martin PE, The connexin mimetic peptide Gap27 increases human dermal fibroblast migration in hyperglycemic and hyperinsulinemic conditions in vitro, J. Cell Physiol 227 (2012) 77–87. [PubMed: 21984074]

[81]. Xu X, Chen C, Akiyama K, Chai Y, Le AD, Wang Z, Shi S, gingivae contain neural-crest- and mesoderm-derived mesenchymal stem cells, J. Dent. Res 92 (2013) 825–832. [PubMed: 23867762]

[82]. Yamada KM, Cukierman E, Modeling tissue morphogenesis and cancer in 3D, Cell 130 (2007) 601–610. [PubMed: 17719539]

[83]. Zhou JZ, Jiang JX, Gap junction and hemichannel-independent actions of connexins on cell and tissue functions-an update, FEBS Lett 588 (2014) 1186–1192. [PubMed: 24434539]

[84]. Schindelin J, Arganda-Carreras I, Frise E, Frise V, Longair M, Pietzsch T, Preibisch S, Rueden C, Saalfeld S, Schmid B, Tinevez JY, White DJ, Hartenstein V, Eliceiri K, Tomancak P, Cardona A, Fiji: an open-source platform for biological-image analysis, Nat. Methods 9 (7) (2012) 676–682. [PubMed: 22743772]

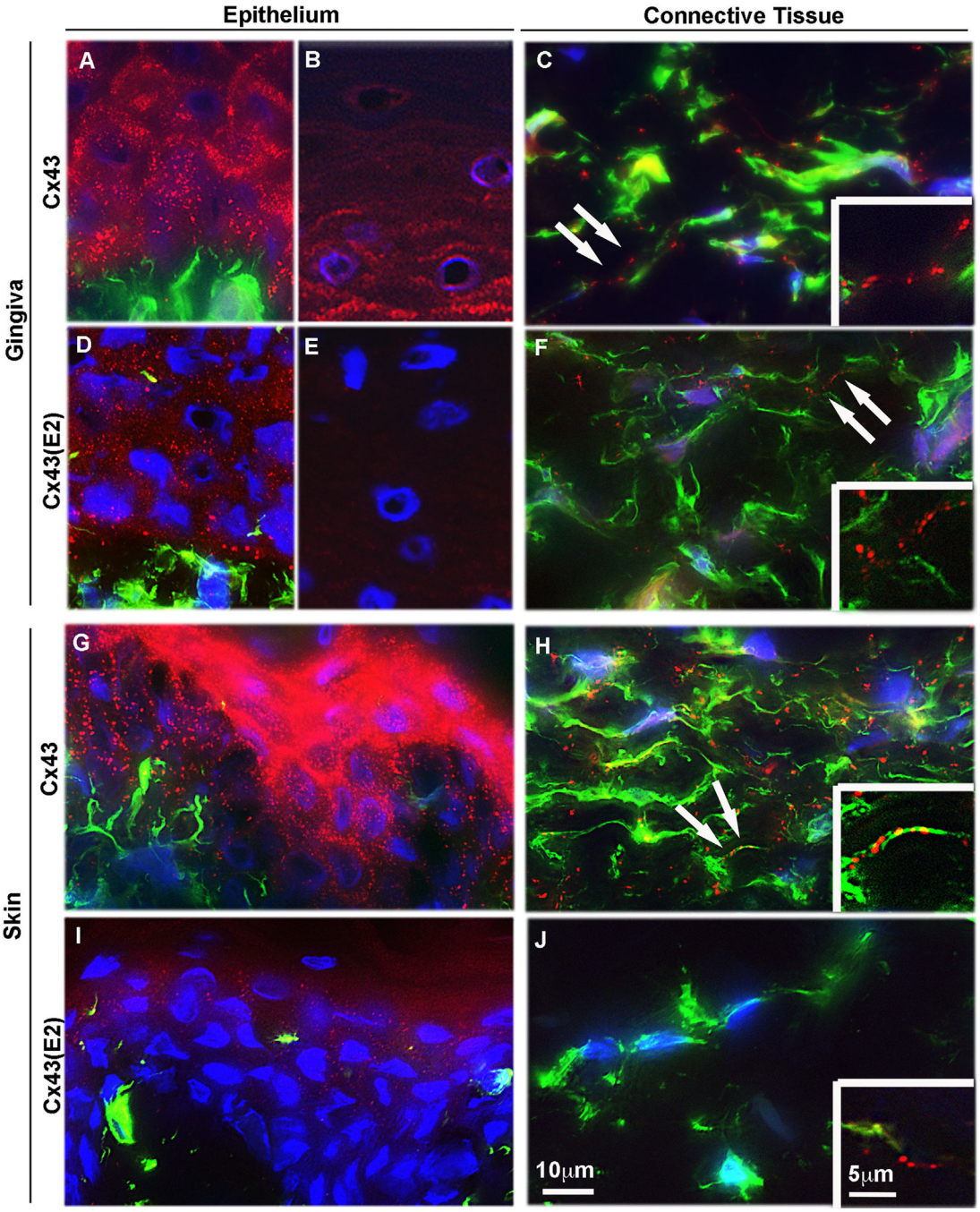

Fig. 1. Localization of Cx43 GJs and HCs in human gingiva and skin *in vivo*.

Representative images of human gingival (A–F) and dermal (G–J) tissue sections double immunostained with an antibody recognizing all forms of the Cx43 molecule (Cx43; A–C, G and H) or only HC-associated Cx43 (Cx43(E2); D–F, I and J) and vimentin (green; a mesenchymal cell marker) in human gingival (A, B, D and E) and dermal (G and I) epithelium, and gingival (C and F) and dermal (H and J) connective tissue. In the gingival epithelium, Cx43 immunostaining localized most abundantly at the cell-cell contacts as plaque-like structures typical to GJs in the basal and spinous layers (A and B). Staining with

the Cx43 HC-specific Cx43(E2) antibody, however, showed localization of Cx43 only in the basal and lower spinous layers (D), with no immunoreactivity at the upper layers of the epithelium (E). In the gingival connective tissue, Cx43 (C) and Cx43(E2) (F) staining was also present as plaque-like staining that mostly localized in the long cellular processes reaching out from the vimentin-positive cells (arrows). In the dermal epithelium (G and I), Cx43 immunostaining (G) localized at the cell-cell contacts with strong immunoreactivity at the upper epithelial layers. Weak staining was noted with Cx43(E2) antibody only at the superficial layers (I). In the dermal connective tissue, Cx43 immunostaining localized abundantly in the long cellular processes (H), similar to the gingival connective tissue (C). Cx43(E2) staining, however, was almost absent from the skin fibroblast processes (J) being only occasionally detected (insert in J). Inserts in (C), (F), (H), and (J) show higher magnification images of Cx43 localization in the long cellular processes. Representative immunostaining images from a minimum of three parallel sections from three individual donors are shown. Nuclear staining (blue) was performed using DAPI.

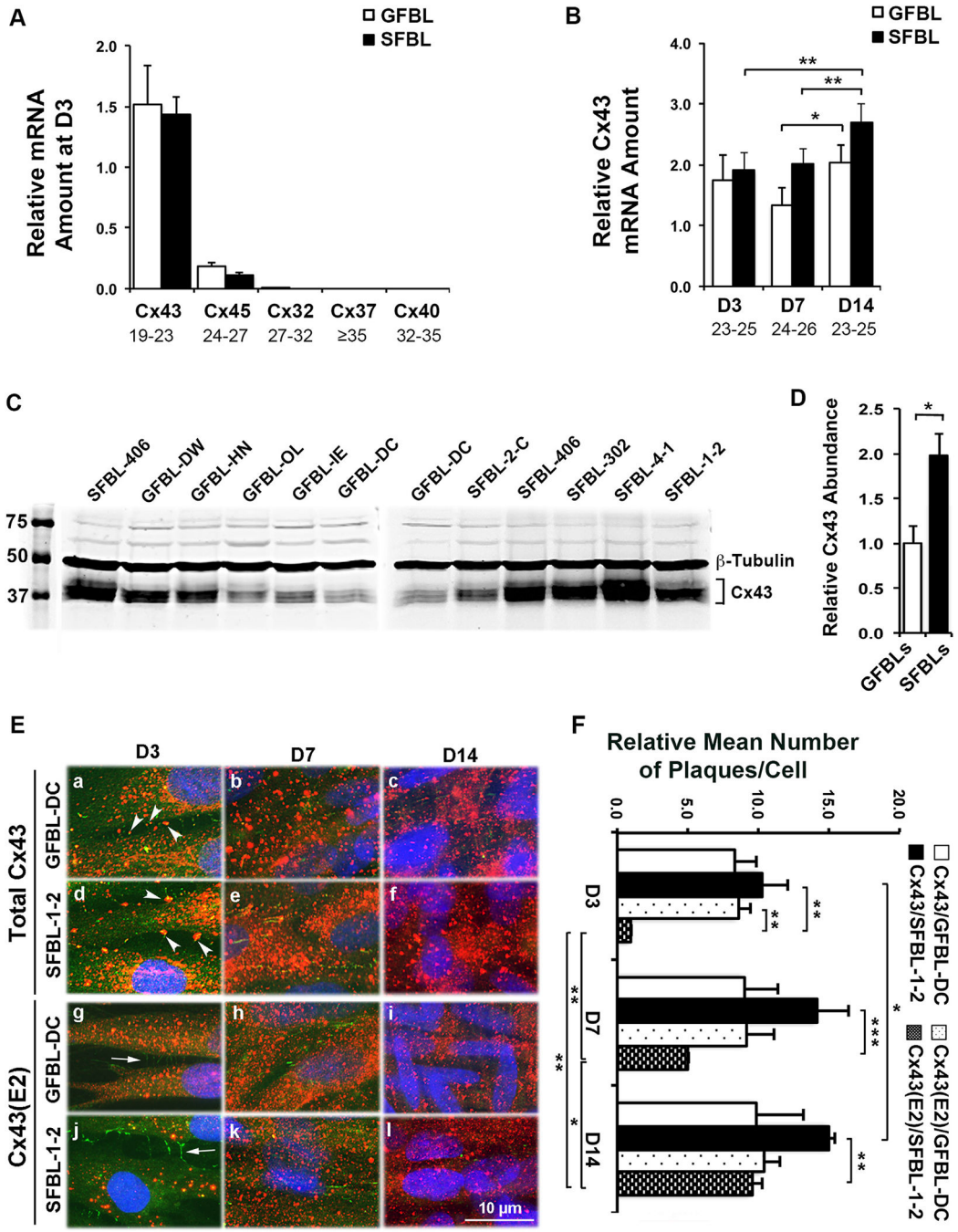

Fig. 2. Cx43 expression and localization in cultured gingival and skin fibroblasts.

(A) Results show qPCR analysis of relative mRNA amount of major Cxs in gingival (GFBLs; GFBL-DW, GFBL-HN, GFBL-OL, GFBL-IE, and GFBL-DC) and skin (SFBLs; SFBL-2-C, SFBL-406, SFBL-302, SFBL-4–1, and SFBL-1–2) fibroblast cultures at day-3 post-seeding. Cx43 was the major Cx expressed in both GFBLs and SFBLs. (B) qPCR analysis of relative Cx43 mRNA amount in GFBLs and SFBLs, 3-, 7-, and 14-days post-seeding. Results represent mean ± s.e.m. from a minimum of three repeated experiments (* $p < 0.05$, ** $p < 0.01$; two-tailed Student's *t*-test). Results in A and B represent mRNA

amount relative to GFBL-DC. Range of the Ct-values obtained from qPCR is indicated below each gene name. (C and D) Western blotting analysis (C) and quantitation (D) of Cx43 in GFBLs and SFBLs day-7 (D7) 3D cultures. SFBLs showed significantly higher abundance of Cx43 compared to GFBLs. Sample loading was normalized for β-Tubulin levels. (E) Representative images from GFBL-DC and SFBL-1–2 day-7 3D cultures double-immunostained for total Cx43 (red) and ZO-1 (green; indicator of cell-cell contacts) (a–f), or HC-associated Cx43 (Cx43(E2); red) and ZO-1 (g–l). (a–f) Cx43 staining was abundantly present in both GFBLs and SFBLs throughout the cell body. In addition, some Cx43 staining colocalized with ZO-1 staining at cell-cell contact areas (arrowheads in a and d), likely representing GJ plaques. (g–l) GFBLs and SFBLs also showed numerous Cx43(E2)-positive plaques that did not colocalize with ZO-1 (arrows in g and j) at the cell-cell contacts, likely representing Cx43 HCs. Nuclear staining (blue) was performed using DAPI. Representative immunostaining images from three parallel samples from two repeated experiments are shown. (F) Quantitation of mean number of total and HC-associated Cx43 plaques per cell over time in culture in GFBL-DC and SFBL-1–2. For quantitation, five standard fields from each coverslip were randomly selected. Cx43-positive plaques were counted in minimum of 100 cells per field. Results are relative to the number of Cx43(E2)-positive plaques in SFBL-1–2 at day-3 post-seeding.

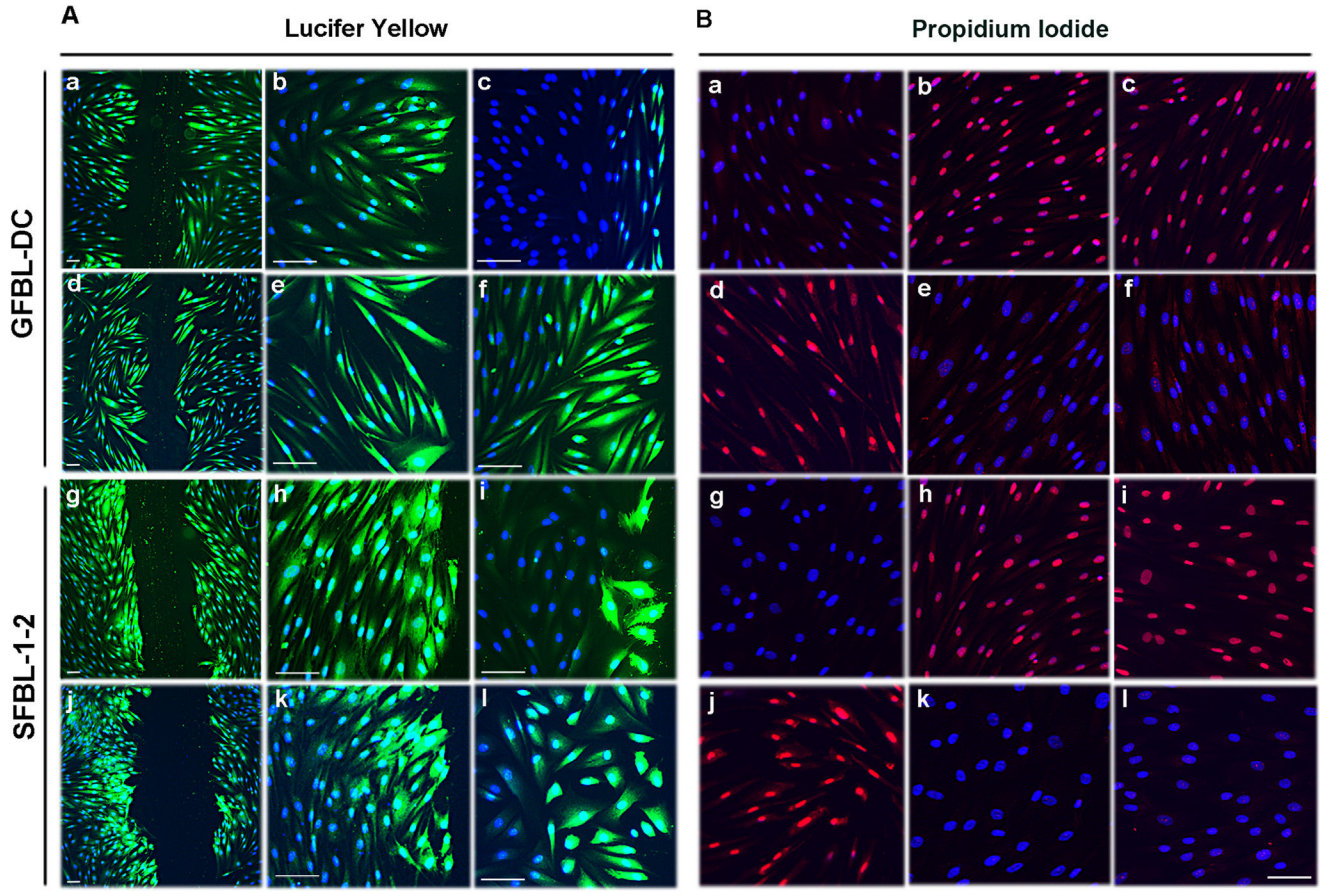

Fig. 3. Gingival and skin fibroblasts have functional Cx43 GJs and HCs.

(A) Assessment of Cx43 GJ function. Confluent day-3 cultures of GFBL-DC (A; a–f) and SFBL-1–2 (A; g–l) were scrape-loaded in DMEM with Lucifer Yellow (green) in the presence of Gap27 control peptide (150 μM) (A; a, b, g, and h), Cx43 mimetic peptide Gap27 (150 μM) (A; c and i), TAT-Gap19 control peptide (400 μM) (A; d, e, j, and k), or TAT-Gap19 (400 μM) (A; f and l), and dye transfer via GJs was followed for 5 min. Gap27 treatment (A; c and i) markedly reduced dye transfer as compared to corresponding control samples (A; a, b, g, and h), while TAT-Gap19 (A; f and l) and corresponding control treatment (A; d, e, j, and k) had no effect. (B) Assessment of Cx43 HC function. Confluent day-3 cultures of GFBL-DC (B; a–f) and SFBL-1–2 (B; g–l) were incubated in DMEM (containing 1.8mM Ca^{+2}) (B; a and g) or low Ca^{+2}-containing medium (EMEM supplemented with 180 nM Ca^{+2}) (B; d and j) in the presence of Cx HC-permeable Propidium Iodide (PI; 2.5 mM, red) for 20 min. Incubation of both GFBLs and SFBLs in EMEM resulted in avid dye uptake (B; d and j), which was blocked when cells were maintained in DMEM (B; a and g). (B; b, c, e, f, h, i, k, and l) Cells were incubated in EMEM and treated with Gap27 control peptide (B; b and h) or Gap27 (150 μM) (B; e and k), TAT-Gap19 control peptide (B; c and i) or TAT-Gap19 (400 μM) (B; f and l). Gap27 (B; e and k) and TAT-Gap19 treatments (B; f and l) markedly blocked Cx43 HC-mediated dye uptake as compared to corresponding control samples (B; b, c, h, I, respectively). Results show representative images from a minimum of two repeated experiments. For the experiments, cells were pretreated with the inhibitors or controls for 1 h before the

experiments. Nuclear staining (blue) was performed using DAPI. Magnification bars in A =30 μm (a, d, g and j) and 50 μm (b, c, e, f, h, i, k and l); in B =50 μm.

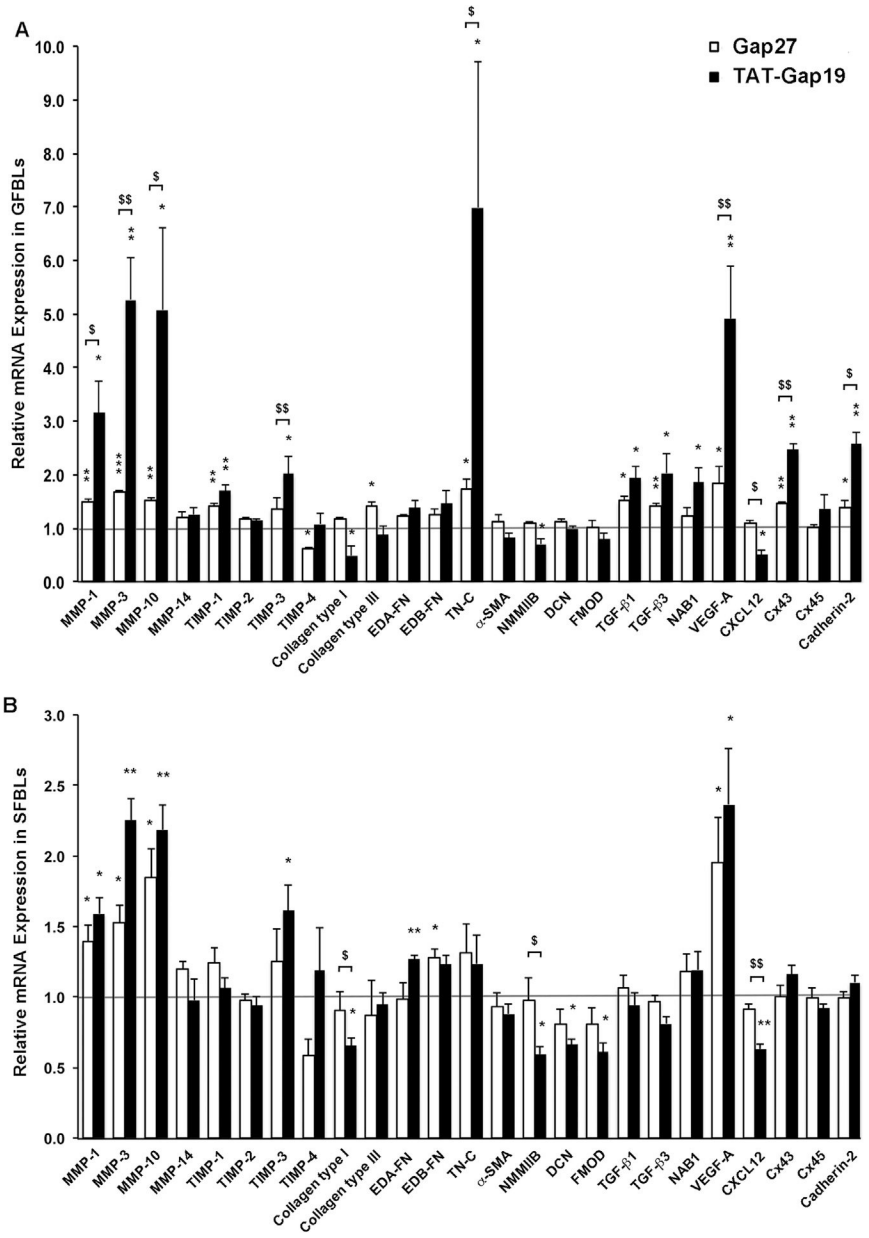

Fig. 4. Gap27 and TAT-Gap19 effect on gene expression response in human gingival and skin fibroblast cultures.

Day-7 3D cultures of GFBLs (A; GFBL-DC, GFBL-IE, and GFBL-DW) and SFBLs (B; SFBL-1–2, SFBL-4–1, and SFBL-302) were serum-starved for 24 h and then treated with Gap27 or control peptide (150 μM), and TAT-Gap19 or control peptide (400 μM) for 24 h, and the expression of a set of genes involved in wound healing was analyzed by qPCR. Results represent mean ± s.e.m. of amount of mRNA relative to control peptide-treated cells. Statistical testing was performed using two-tailed Student's *t*-test by comparison between Gap27- or TAT-Gap19-induced gene expression changes ($ $p < 0.05$, $ $ $p < 0.01$), or relative to the corresponding control peptide-treated samples, respectively (* $p < 0.05$, ** $p < 0.01$, *** $p < 0.001$). Horizontal line (= 1) indicates relative amount of mRNA for the control peptide-treated samples. EDA-FN: Extra Domain A-Fibronectin; EDB-FN: Extra

Domain B-Fibronectin; TN-C: Tenascin-C; α-SMA: α-Smooth Muscle Actin; NMMIIB: Non-Muscle Myosin IIB; DCN: Decorin; FMOD: Fibromodulin; NAB1: NGFI-A Binding Protein-1; VEGF-A: Vascular Endothelial Growth Factor-A.

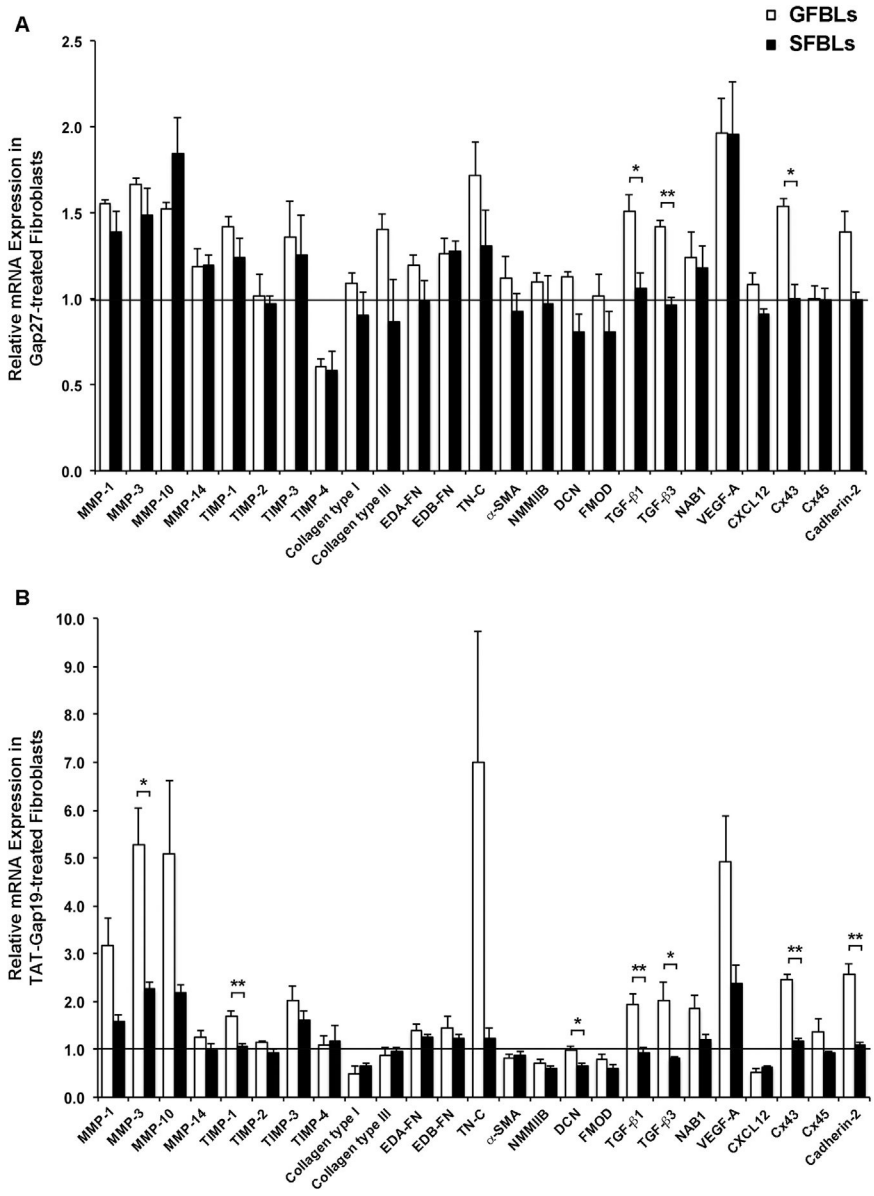

Fig. 5. Gene expression response to Gap27 or TAT-Gap19 treatment in human gingival and skin fibroblast cultures.

Day-7 3D cultures of GFBLs (GFBL-DC, GFBL-IE, and GFBL-DW) and SFBLs (SFBL-1–2, SFBL-4–1, and SFBL-302) were treated with (A) Gap27 or control peptide (150 μM), or (B) TAT-Gap19 or control peptide (400 μM) for 24 h, and the expression of a set of genes involved in wound healing was analyzed by qPCR. Results represent mean ± s.e.m. of amount of mRNA relative to control peptide-treated cells (= 1). Statistical testing was performed between GFBLs and SFBLs for each peptide treatment (* $p < 0.05$, ** $p < 0.01$; two-tailed Student's *t*-test). Horizontal line (= 1) indicates relative amount of mRNA for the control peptide-treated samples in both GFBLs and SFBLs. EDA-FN: Extra Domain A-Fibronectin; EDB-FN: Extra Domain B-Fibronectin; TN-C: Tenascin-C; α-SMA: α-Smooth

Muscle Actin; NMMIIB: Non-Muscle Myosin IIB; DCN: Decorin; FMOD: Fibromodulin; NAB1: NGFI-A Binding Protein-1; VEGF-A: Vascular Endothelial Growth Factor-A.

Table 1

Regulation of the expression of wound healing-associated genes by Cx43 GJ and HC blocking peptides in gingival and skin fibroblasts. The table summarizes data from Fig. 4. Genes are indicated based on whether their expression was significantly ($p < 0.05$; two-tailed Student's *t*-test) changed only by Gap27, only by TAT-Gap19, by both Gap27 and TAT-Gap19, or genes that were not regulated by Gap27 and TAT-Gap19 relative to corresponding controls. For the experiment, day-7 3D cultures from three parallel GFBL and SFBL strains were treated with Gap27 (150 μM), TAT-Gap19 (400 μM) or corresponding control peptides for 24 h. Results are from qPCR analysis of mRNA amount relative to control peptide-treated samples. Genes regulated by different mechanisms in GFBLs and SFBLs are bolded. Coll I: Collagen type I; Coll III: Collagen type III; EDA-FN: Extra Domain A-Fibronectin; EDB-FN: Extra Domain B-Fibronectin; TN-C: Tenascin-C; α-SMA: α-Smooth Muscle Actin; NMMIIB: Non-Muscle Myosin IIB, DCN: Decorin; FMOD: Fibromodulin; NAB1: NGFI-A Binding Protein-1; VEGF-A: Vascular Endothelial Growth Factor-A.

Genes not regulated by Gap27 and TAT-Gap19		**Genes regulated by Gap27 only**		**Genes regulated by TAT-Gap19 only**		**Genes regulated by both Gap27- and TAT-Gap19**	
GFBLs	**SFBLs**	**GFBLs**	**SFBLs**	**GFBLs**	**SFBLs**	**GFBLs**	**SFBLs**
MMP-14	MMP-14	**TIMP-4**	**EDB-FN**	TIMP-3	TIMP-3	MMP-1	MMP-1
TIMP-2	TIMP-2	**Coll III**		Coll I	Coll I	MMP-3	MMP-3
α-SMA	α-SMA			NMMIIB	NMMIIB	MMP-10	MMP-10
Cx45	Cx45			CXCL12	CXCL12	VEGF-A	VEGF-A
EDA-FN	**TIMP-1**			**NAB1**	**EDA-FN**	**TIMP-1**	
EDB-FN	**TIMP-4**				**DCN**	**TN-C**	
DCN	**Coll III**				**FMOD**	**TGF-β1**	
FMOD	**TN-C**					**TGF-β3**	
	TGF-β1					**Cx43**	
	TGF-β3					**Cadherin-2**	
	NAB1						
	Cx43						
	Cadherin-2						